


# A new phenothiazine-based fluorescence sensor for imaging $\text{Hg}^{2+}$ in living cells

Yucheng Sun<sup>1</sup> | Lizhen Wang<sup>2</sup> | Jianhua Zhou<sup>1</sup> | Dawei Qin<sup>1</sup> |  
Hongdong Duan<sup>1</sup> 

<sup>1</sup>School of Chemistry and Pharmaceutical Engineering, Qilu University of Technology (Shandong Academy of Sciences), Ji'nan, Shandong Province, 250353, China

<sup>2</sup>Biology Institute, Qilu University of Technology (Shandong Academy of Sciences), Ji'nan, Shandong Province, 250014, China

## Correspondence

Hongdong Duan, School of Chemistry and Pharmaceutical Engineering, Qilu University of Technology (Shandong Academy of Sciences), Ji'nan, Shandong Province, China 250353.  
Email: hdduan67@163.com

## Funding information

Major Science and Technology Innovation Project of Shandong Province, Grant/Award Number: 2018 CXGC1107; Shandong Provincial Natural Science Foundation of China, Grant/Award Numbers: ZR2018PB007 and, ZR2017LC005

A new phenothiazine-based sensor PHE-Ad for monitoring  $\text{Hg}^{2+}$  has been designed and synthesized based on the intramolecular charge transfer (ICT) mechanism. The probes were characterized by FTIR,  $^1\text{H}$  NMR, and HRMS, and their optical properties were detected by UV and FL. It's showed the probes detection of  $\text{Hg}^{2+}$  compared to other metal ions ( $\text{Mg}^{2+}$ ,  $\text{Cu}^{2+}$ ,  $\text{Hg}^{2+}$ ,  $\text{Ag}^+$ ,  $\text{Co}^{2+}$ ,  $\text{Cr}^{3+}$ ,  $\text{Al}^{3+}$ ,  $\text{Ni}^{2+}$ ,  $\text{Zn}^{2+}$ ,  $\text{Ca}^{2+}$ ,  $\text{Fe}^{3+}$ ,  $\text{Fe}^{2+}$ ,  $\text{K}^+$ ,  $\text{Na}^+$ , and  $\text{Cd}^{2+}$ ) based on the test results. Besides, the detection limits were determined to be  $2.12 \times 10^{-8}$  M through the standard curve plot. In addition, sensor PHE-Ad shows high selectivity and sensitivity for  $\text{Hg}^{2+}$  with a fast response in a suitable pH range. Furthermore, taking into account its good "turn-on" fluorescent sensing behavior and low cell cytotoxicity, PHE-Ad was successfully applied to detect and image  $\text{Hg}^{2+}$  in real water samples and living cells, which shows great potentials for application in environmental and biological systems.

## KEYWORDS

cell image, fluorescence probe,  $\text{Hg}^{2+}$ , ICT, pH

## 1 | INTRODUCTION

Mercury is a heavy metal that is easily absorbed by the body in the form of ions and is difficult to degrade in living organisms.<sup>[1–3]</sup>  $\text{Hg}^{2+}$  easily accumulates in the human body through the food chain, causing a series of health problems,<sup>[4,5]</sup> such as digestion, heart, kidney, DNA, mitotic damage and permanent damage to the nervous system.<sup>[6–8]</sup> Mercury is widely used in industrial production,<sup>[9]</sup> and the production volume has increased sharply.<sup>[10]</sup> A large amount of mercury-containing wastes have been discharged to the environment,<sup>[11]</sup> causing mercury pollution in the environment to become increasingly serious.<sup>[12–14]</sup> Therefore, finding an efficient and simple

method for detecting  $\text{Hg}^{2+}$  is of great significance to both human health<sup>[15]</sup> and environmental protection.<sup>[16,17]</sup>

The fluorescence intensity of the fluorescent probe based on the fluorescence on–off sensing mechanism is easily affected by the external environment,<sup>[18]</sup> such as temperature, excitation power,<sup>[19]</sup> and medium properties.<sup>[20,21]</sup> The thiol fluorescent probe not only has the advantages of high selectivity and high sensitivity,<sup>[22]</sup> but also its fluorescence intensity is not easily affected by the external environment,<sup>[23]</sup> and it is prone to deprotection reactions to detect mercury ions with the naked eye.<sup>[24]</sup> Therefore, based on these advantages of the deprotection thioacetal fluorescent probe,<sup>[25,26]</sup> a phenothiazine derivative thioacetal fluorescent probe was designed and synthesized.<sup>[27,28]</sup>

Phenothiazine is a compound containing S and N heterocycles,<sup>[29]</sup> which has applications in different chemical fields such as dyes,<sup>[30]</sup> probes, drugs and electrochemistry.<sup>[31]</sup> Phenothiazine derivatives can be used as raw materials for the synthesis of fluorescent probes<sup>[32,33]</sup> due to their excellent fluorescence properties, regular structure, better hole transport ability transportability, and lower ionization potential.<sup>[34]</sup> In this paper, phenothiazine was used as a raw material to react with ethyl mercaptan<sup>[35]</sup> after inserting ethyl and aldehyde groups to synthesize a thiol probe with good selectivity and high sensitivity to mercury ions.<sup>[1,36]</sup>

## 2 | EXPERIMENT PROCEDURE

### 2.1 Reagents, materials and apparatus

The solvents and drugs used in the experiments were all analytical grade and obtained from commercial sources. The <sup>1</sup>H NMR (400 MHz) is measured on a Bruker AV-400 spectrometer with DMSO-*d*<sub>6</sub> used as the solvent and tetramethyl silane (TMS) as the internal standard. Infrared measurements were performed using a KBr pellet technique on a Bruker ALPHA FT-IR spectrometer in the 4,000–400 cm<sup>−1</sup> region. High resolution mass spectrometry (HRMS) was performed using an Agilent 6,510 precision mass Q-TOF LC/MS system. Fluorescence spectra were recorded on a Hitachi FI-4,600 fluorescence spectrophotometer with a scan rate of 2,400 nm/min. Ultraviolet–visible (UV–Vis) absorption were measured on SHIMADZU UV-2600. All experiments were performed at room temperature.

### 2.2 | General procedure for the spectra measurement

An ethanol solution with a concentration of  $1.0 \times 10^{-3}$  mol/l compound and a concentration of  $1.0 \times 10^{-3}$  mol/L Mg<sup>2+</sup>, Cu<sup>2+</sup>, Hg<sup>2+</sup>, Ag<sup>+</sup>, Co<sup>2+</sup>, Cr<sup>3+</sup>, Al<sup>3+</sup>, Ni<sup>2+</sup>, Zn<sup>2+</sup>, Ca<sup>2+</sup>, Fe<sup>3+</sup>, Fe<sup>2+</sup>, K<sup>+</sup>, Na<sup>+</sup>, and Cd<sup>2+</sup> metal ion solution were prepared. Using a pipette, removing 1 ml of the compound's absolute ethanol solution and metal ion aqueous solution into 100 ml volumetric flasks, then diluting it with a mixed solution of absolute ethanol: distilled water (1: 1) to close to the scale line, and then use a dropper to make up the volume. The mixed solution was used as the stock solution for the following experiments.<sup>[37–39]</sup>

### 2.3 | Synthesis of sensor PHE-ad

Compounds 1 and 2 were prepared in accordance with the literature.<sup>[40]</sup> Weigh out the compound 2 (0.205 g, 1.0 mmol) and ethyl mercaptan (0.248 g, 2.0 mmol) in

20 ml of dichloromethane. The catalyst ether boron trifluoride (0.10 ml, 0.79 mol) was slowly added dropwise to the above system at 0 °C, and the reaction was stirred overnight at the above temperature. After the reaction was completed, 10 ml of methanol was added for crystallization, and pale-yellow crystals were formed. The crude compound was obtained by suction filtration. Dichloromethane was separated and purified by silica gel column chromatography: petroleum ether (4:1) as eluent, and evaporated to dryness on a rotary evaporator to obtain the PHE-Ad.(0.264 g, yield 69.9%). MP 81.2–81.7 °C; FTIR (KBr, cm<sup>−1</sup>) ν = 1,598, 1,467 (C=C), 1,247 (C–N), 1,132 (C–S). <sup>1</sup>H NMR (400 MHz, DMSO) δ 7.29–7.12 (m, 4H, ArH), 7.04–6.90 (m, 3H, ArH), 5.11 (s, 1H, –CH), 3.90 (q, J = 6.8 Hz, 2H, –CH<sub>2</sub>), 2.69–2.37 (m, 4H, –CH<sub>2</sub>), 1.29 (t, J = 6.9 Hz, 3H, –CH<sub>3</sub>), 1.15 (t, J = 7.4 Hz, 6H, –CH<sub>3</sub>). HRMS (ESI) m/z calcd for C<sub>19</sub>H<sub>23</sub>NS<sub>3</sub> [M + H]<sup>+</sup>: 361.5877; Found 362.5882. Elemental analysis was performed on the proportions of the C, H, N, and S elements of the compound with molecular weight by a VarioEL III elemental analyzer. The measured values of the C, H, S and N elements in the compound PHE-Ad were 63.58%, 7.42%, 3.67%, 25.51%, and the theoretical values were 63.61%, 7.21%, 3.71%, 25.47%. After comparison, it was found that the values were very close, and the error was negligible. Therefore, the test results further proved that the compound (PHE-Ad) had been successfully synthesized.

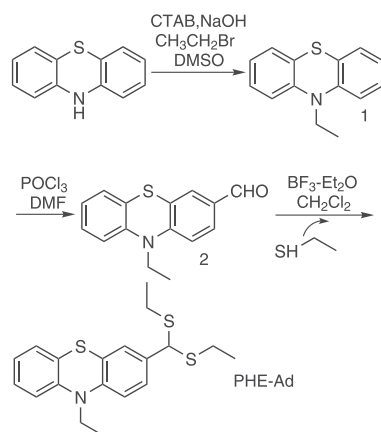
### 2.4 | Fluorescence imaging of Hg<sup>2+</sup> in living cells

HeLa cells were cultured in DMEM, and 10% FBS was added at 37 °C (below 5% CO<sub>2</sub>) for cell imaging experiments. First, live HeLa cells and sensor PHE-Ad (10 μm) were cultured in cell culture medium at 37 °C for 1 hr, washed with water PBS buffer (pH = 7.4) for three times, and then imaged. Second, Hg<sup>2+</sup> (10 μm) was added to the pre-cultured cells of the PHE-Ad, incubated at 37 °C for 30 min, washed three times with PBS, and then imaged. After 60 min, imaging the cells that loaded Hg<sup>2+</sup> again were detected under CLSM.

## 3 | RESULTS AND DISCUSSION

### 3.1 | Design and synthesis of PHE-ad

As described in Scheme 1, compound PHE-Ad was facilely synthesized from compound 2 and ethanethiol. Compound 2 could be synthesized according to methods in the literature. The structure of PHE-Ad was well confirmed by <sup>1</sup>H NMR, FTIR and Elemental analysis. Our design strategy is



**SCHEME 1** The synthetic route of sensor PHE-Ad

based on well-known  $\text{Hg}^{2+}$  promoted thioacetal desulfurization reaction is corresponding aldehyde.

### 3.2 | UV-vis spectral analysis of compound PHE-ad

The purpose of test the detection ability of synthetic probe PHE-Ad for metal ions, a series of metal ion recognition experiments were performed on a dual-beam UV-visible spectrophotometer model TU-1900. The blank sample PHE-Ad has an obvious UV-visible absorption band near 310 nm. After adding  $\text{Hg}^{2+}$  to the blank sample PHE-Ad, there is an obvious UV-visible absorption band near 390 nm, and the UV-visible absorption

band shows a clear red shift. When other metal ions were added, there was no obvious UV-visible absorption band around 390 nm, however, the same maximum absorption wavelength appeared around 310 nm as the blank sample. Based on the analysis of the above phenomena, it is preliminarily judged that the compound PHE-Ad has good selectivity for metal ions  $\text{Hg}^{2+}$  (Figure 1).

### 3.3 | Compound PHE-ad color comparison experiment

The selectivity of the compound PHE-Ad to metal ions was detected through a color contrast experiment. The concentration of the mixed solution of the compound and metal ions was  $1.0 \times 10^{-5}$  mol/l. The color of the mixed solution changed significantly from colorless to yellow after adding the metal ion  $\text{Hg}^{2+}$ , but no other color change occurred when other metal ions were added to the blank compound (Figure 2). This result indicates that the compound PHE-Ad is accompanied by a significant color change when the deprotection reaction occurs. The presence of  $\text{Hg}^{2+}$  can be detected with the naked eye.

### 3.4 | Calculation of association constants of compounds PHE-ad

The dual-beam ultraviolet-visible spectrophotometer was used to determine the Job's curve to determine the stoichiometry of the compound PHE-Ad and metal ions. Pipette 0.1, 0.2, 0.3, 0.4, 0.5, 0.6, 0.7, 0.8, 0.9 ml of a

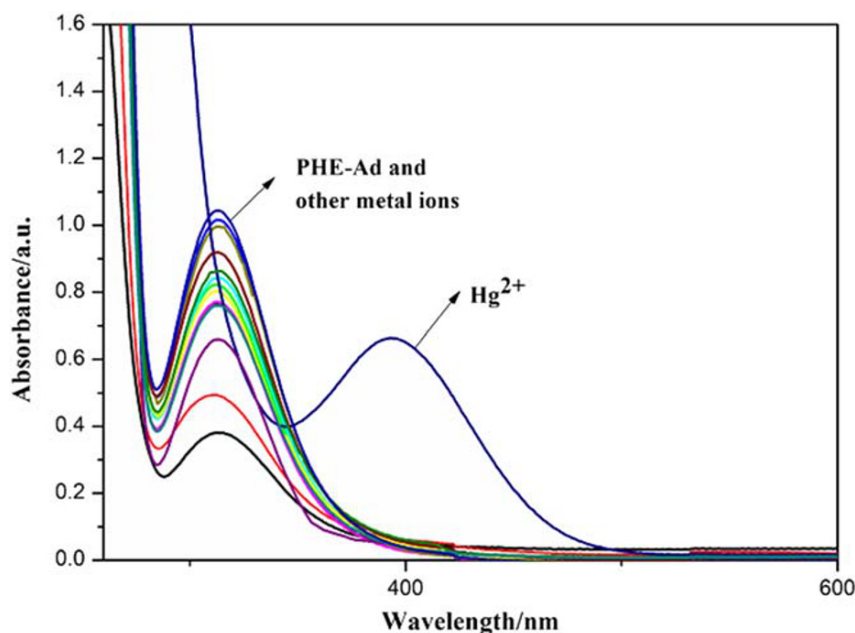


**FIGURE 1** Ultraviolet absorption spectrum of compound PHE-Ad and metal ion mixed Solution

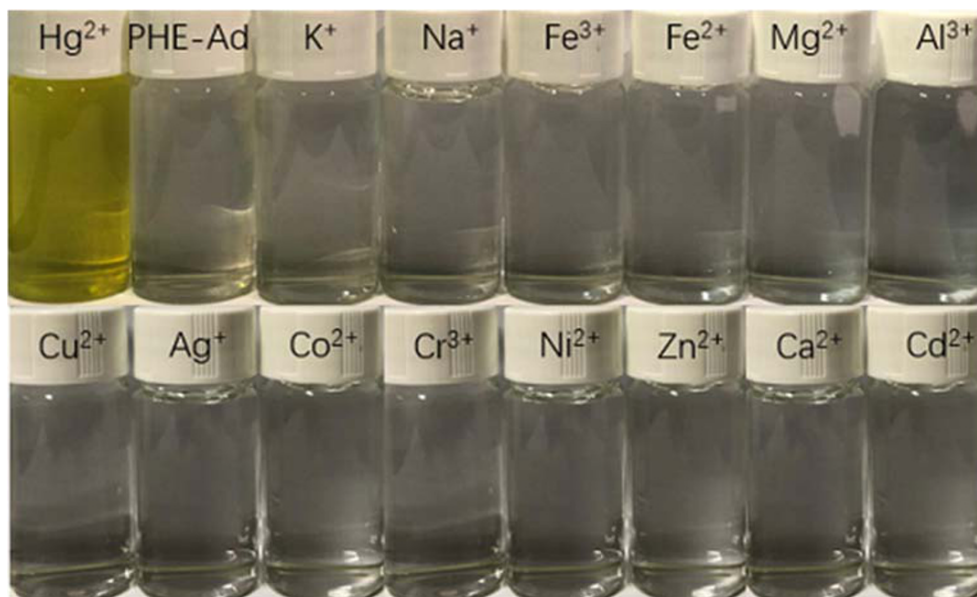


**FIGURE 2** Color contrast chart of compound PHE-Ad and metal ion mixed solution under visible light

compound solution at a concentration of  $1.0 \times 10^{-3}$  mol/l into a 100 ml volumetric flask. Then, 0.9, 0.8, 0.7, 0.6, 0.5, 0.4, 0.3, 0.2, and 0.1 ml of  $\text{Hg}^{2+}$  aqueous solution with a concentration of  $1.0 \times 10^{-3}$  mol/l were added to the above volumetric flasks in order. The total volume of the compound solution and the metal ion solution is 1 ml. Dilute to a tick mark with a mixed solution of absolute ethanol: water (1:1), and mix up and down. The ultraviolet absorption intensity is strongest when the compound concentration and metal ion concentration are both  $0.5 \times 10^{-5}$  mol/l (Figure 3). The results show that the chemical binding number of the compound with  $\text{Hg}^{2+}$  is 1: 1, and the association constant of the compound and  $\text{Hg}^{2+}$  calculated according to the Benesi-Hildebrand equation is  $1.56 \times 10^{-5} \text{ M}^{-1}$ .

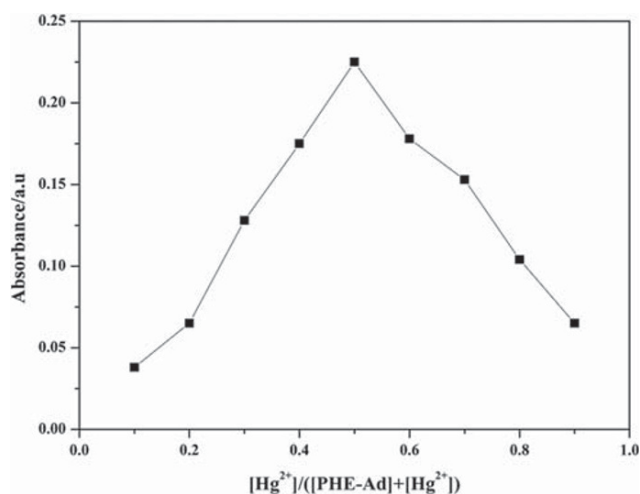


**FIGURE 3** Job's graph of compound PHE-Ad

### 3.5 | Compound PHE-ad fluorescence spectral analysis

In order to study the fluorescence properties of the compounds, a model of F-4600 fluorescence spectrophotometer was used for a compound with a concentration of  $1.0 \times 10^{-5}$  mol/l and a series of metal ions  $\text{Mg}^{2+}$ ,  $\text{Cu}^{2+}$ ,  $\text{Hg}^{2+}$ ,  $\text{Ag}^{+}$ ,  $\text{Co}^{2+}$ ,  $\text{Cr}^{3+}$ ,  $\text{Al}^{3+}$ ,  $\text{Ni}^{2+}$ ,  $\text{Zn}^{2+}$ ,  $\text{Ca}^{2+}$ ,  $\text{Fe}^{3+}$ ,  $\text{Fe}^{2+}$ ,  $\text{K}^{+}$ ,  $\text{Na}^{+}$ , and  $\text{Cd}^{2+}$  was tested for fluorescence performance. When  $\text{Hg}^{2+}$  is added to a blank sample of the compound, there is an obvious fluorescence emission band at 610 nm when the excitation wavelength is 390 nm. However, after adding other metal ions to the blank sample, no fluorescence emission band was found at 610 nm, and only a significant fluorescence emission band was observed around 455 nm (Figure 4). The above results indicate that the fluorescence emission of the compound shows a significant red shift after adding  $\text{Hg}^{2+}$ , and the compound has a high selectivity for the metal ion  $\text{Hg}^{2+}$ . Using rhodamine B as a reference, the fluorescence quantum yield of the compound was calculated to be 0.115 according to the formula, and the results show that the compound has some potential application value.

### 3.6 | Sensitivity study

So as to study the sensitivity of the compounds to detect  $\text{Hg}^{2+}$ , a series of fluorescence titration experiments were performed. As the concentration of the metal ion in the blank compound increases (0-14  $\mu\text{M}$ ), the intensity of the fluorescence emission peak at 610 nm gradually increases. When the concentration reaches 10  $\mu\text{M}$ , the



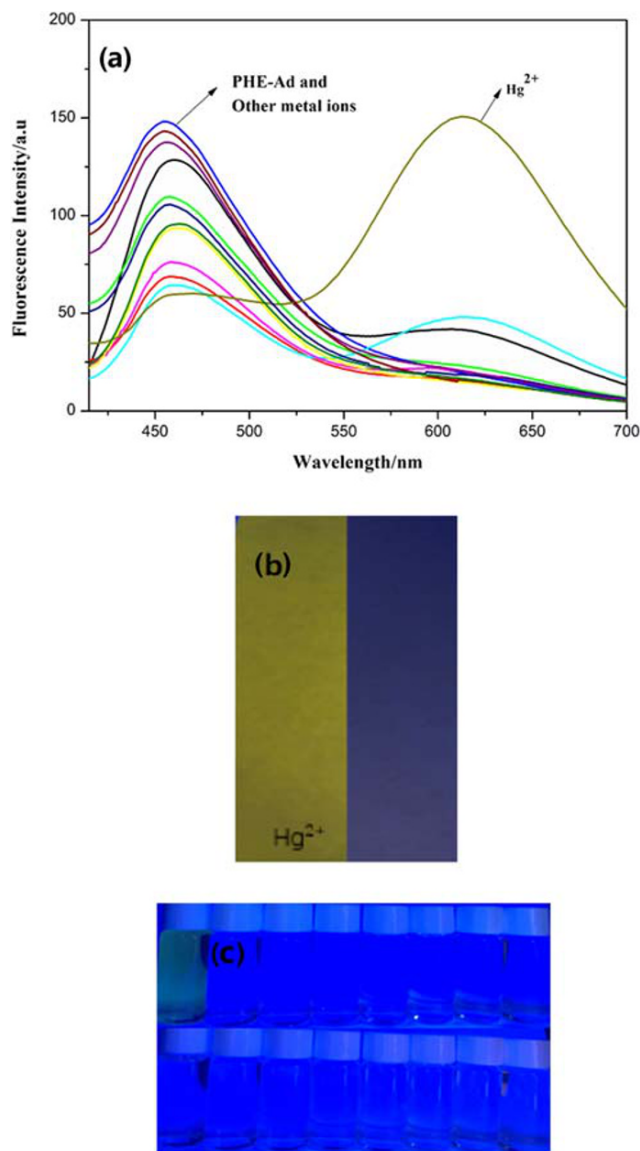


**FIGURE 4** a-c (a) Compound PHE-Ad fluorescence emission spectrum (b) Fluorescence emission of PHE-Ad in solution (c) Fluorescence emission of PHE-Ad on test paper

fluorescence emission intensity reaches a plateau and the fluorescence intensity does not change (Figure 5). The above results show that the reaction ratio of this compound to  $\text{Hg}^{2+}$  is 1:1. The fluorescence emission intensity of the compound PHE-Ad has a good linear relationship with the  $\text{Hg}^{2+}$  concentration ( $R^2 = 0.9921$ ). According to the formula  $\text{LOD} = 3\sigma/k$ , the detection limit of the compound for detecting  $\text{Hg}^{2+}$  can be as low as  $2.12 \times 10^{-8}$  mol/l, indicating that the compound can detect  $\text{Hg}^{2+}$  with high sensitivity (Figure 6).

### 3.7 | Reaction mechanism studies

Since the sulfur-philicity of  $\text{Hg}^{2+}$  can induce the deprotection reaction of thiol to generate the corresponding

aldehyde compound 2-aldehyde-10-ethylphenothiazine, other metal ions cannot induce the deprotection reaction, therefore, this process is used for A fluorescent probe for detecting  $\text{Hg}^{2+}$  based on a deprotection reaction. During this reaction, 10-ethylphenothiazine was used as an electron donor, and 2- (demethylation) -methine was used as a weak electron donor to form an electron donor. The donor system prevents the intra-molecular charge transfer process (ICT). When  $\text{Hg}^{2+}$  was added to the blank sample of the compound, a deprotection reaction occurred, and an electron-deficient aldehyde group, namely 2-aldehyde group-10-ethyl compound, was formed. The aldehyde group was used as the electron acceptor 10-ethylphenothiazine. Partially acting as an electron donor, the donor-acceptor system opens the intra-molecular charge transfer process (ICT), as a result, the UV-visible absorption band and fluorescent emission band are red-shifted (Figure 7).

In order to prove the detection mechanism of the compound, a series of tests were performed on the product after adding  $\text{Hg}^{2+}$  to the deprotection reaction in the blank sample. First, the infrared spectrum of the compound after the reaction was measured on a Bruker TENSOR27 infrared spectrometer using KBr tableting. As shown in Figure 8, Figure (a) is the infrared spectrum of the compound blank, and Figure (b) is the infrared spectrum of the compound blank after adding  $\text{Hg}^{2+}$ . It can be seen from the Figure that after the addition of  $\text{Hg}^{2+}$ , a new absorption peak appeared at  $1680 \text{ cm}^{-1}$ , and it can be seen from the literature that this peak is an aldehyde group absorption peak. The above analysis results indicate that the thiol group on 2- (demethylation) -methine-10-ethylphenothiazine has successfully deprotected under the action of  $\text{Hg}^{2+}$ , and the corresponding pheophytin aldehydes of azine derivatives (Figure 8).

Then, in order to further prove the deprotection reaction between the compound and  $\text{Hg}^{2+}$ , a nuclear magnetic titration experiment was performed.  $\text{Hg}^{2+}$  was added to a blank sample with a concentration of  $1.0 \times 10^{-5}$  mol/L in the mixed solution (Figure 9). After the reaction was completed, a large amount of distilled water was added to precipitate the reaction product, which was then filtered and dried under vacuum to obtain the compound.<sup>1</sup>  $^1\text{H}$ NMR spectra of the compounds were measured using deuterated DMSO as the solvent. It can be seen from the Figure that the proton hydrogen signal peaks attributed to  $-\text{CH}$  at 5.17 ppm, 2.91 ppm, 2.73 ppm, 1.97 ppm, and 1.55 ppm, the proton hydrogen signal peaks attributed to  $-\text{CH}_2-\text{CH}_2-\text{CH}_2-$  are completely disappearing. However, the signal peak attributed to  $-\text{CHO}$  appeared at 9.80 ppm, which was consistent with the  $^1\text{H}$ NMR spectrum of the compound

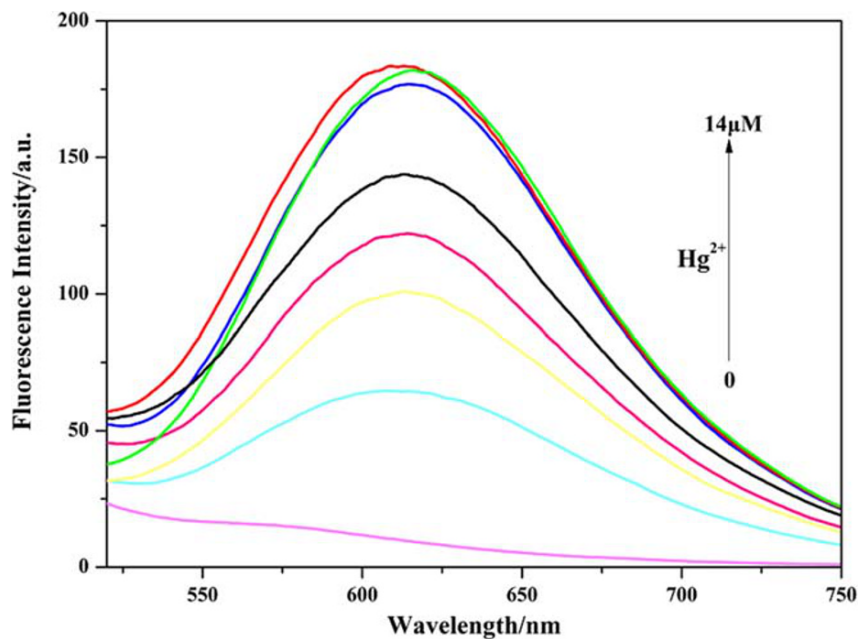


**FIGURE 5** Fluorescence emission spectrum of compound PHE-Ad fluorescence titration

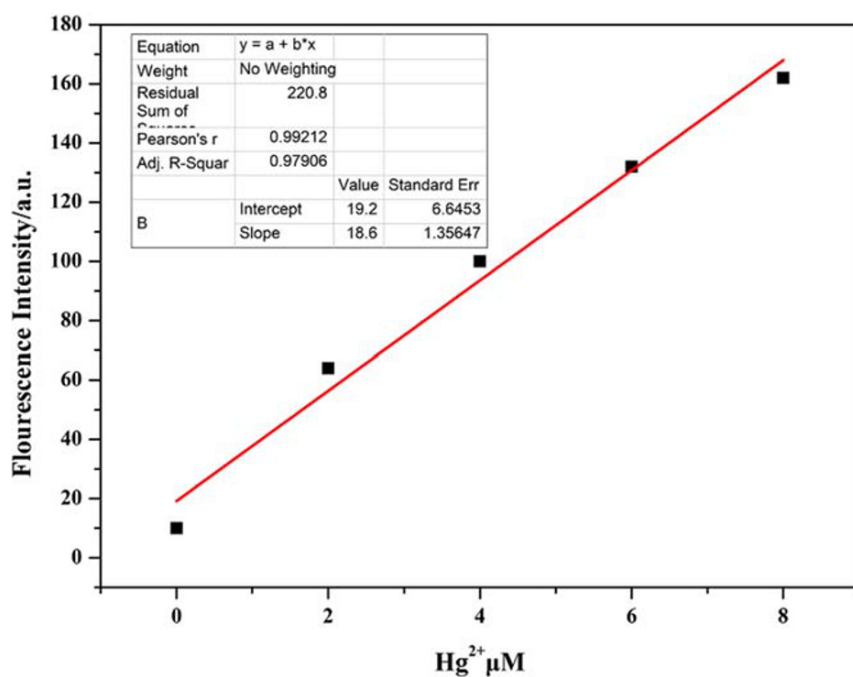


**FIGURE 6** The linear relationship between PHE-Ad fluorescence emission intensity and  $\text{Hg}^{2+}$  ion concentration

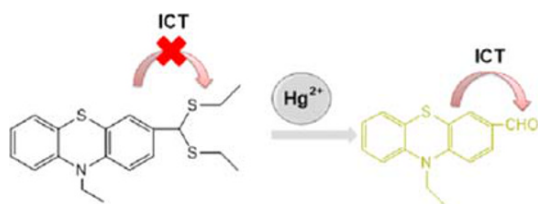


**FIGURE 7** Compound PHE-Ad detection mechanism diagram

2-aldehyde--10-ethylphenothiazine. The above results show that the compound and  $\text{Hg}^{2+}$  successfully deprotected the compound 2-aldehyde- 10-ethylphenothiazine.

According to the above research results, as shown in Figure.7, the reaction mechanism between PHE-Ad and  $\text{Hg}^{2+}$  occurs. The ionophilicity of  $\text{Hg}^{2+}$  can induce the deprotection reaction of thioaldehyde to form the corresponding aldehyde compound 2. In the course of

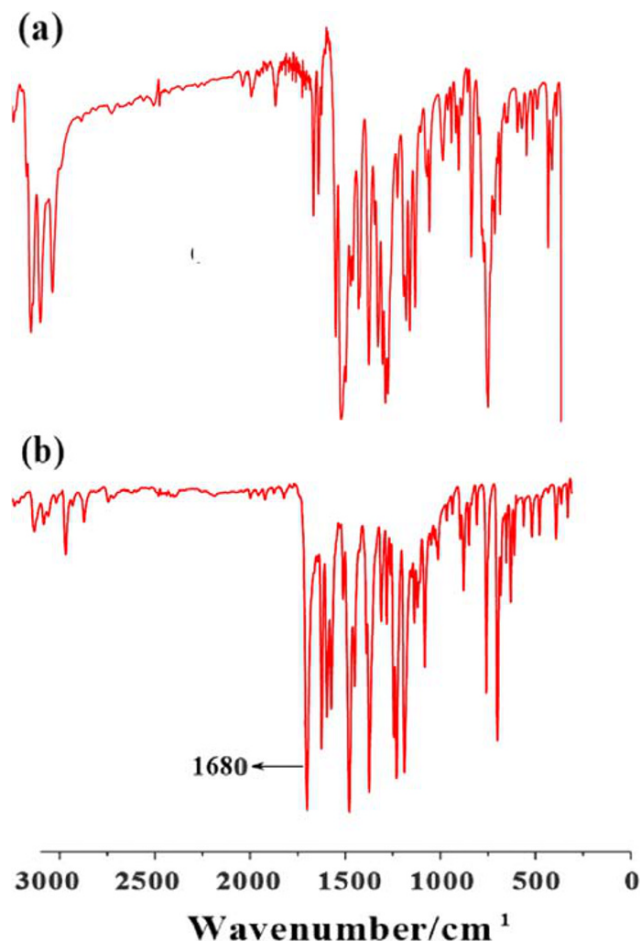


**FIGURE 8** The infrared spectrum of the product of the deprotection reaction between the compound PHE-Ad and Hg<sup>2+</sup>

this reaction, the deprotection reaction occurs with the addition of Hg<sup>2+</sup>, forming a donor-acceptor system and opening up the intramolecular charge transfer process (ICT). Therefore, studies have shown that PHE-Ad can be used as the high selectivity for Hg<sup>2+</sup>. The fluorescence-on sensor is of great use for the selective detection of mercury ions in the environment and biological systems.

### 3.8 | Competition studies

The compound is subject to interference from other metal ions when detecting metal ions. In order to study the anti-interference performance of the compound when detecting Hg<sup>2+</sup>, a series of competitive experiments were performed. A mixed solution of Mg<sup>2+</sup>, Cu<sup>2+</sup>, Hg<sup>2+</sup>, Ag<sup>+</sup>, Co<sup>2+</sup>, Cr<sup>3+</sup>, Al<sup>3+</sup>, Ni<sup>2+</sup>, Zn<sup>2+</sup>, Ca<sup>2+</sup>, Fe<sup>3+</sup>, Fe<sup>2+</sup>, K<sup>+</sup>, Na<sup>+</sup>, BSA and Cd<sup>2+</sup> and compounds at a concentration of  $1.0 \times 10^{-5}$  mol/l was tested for fluorescence. The

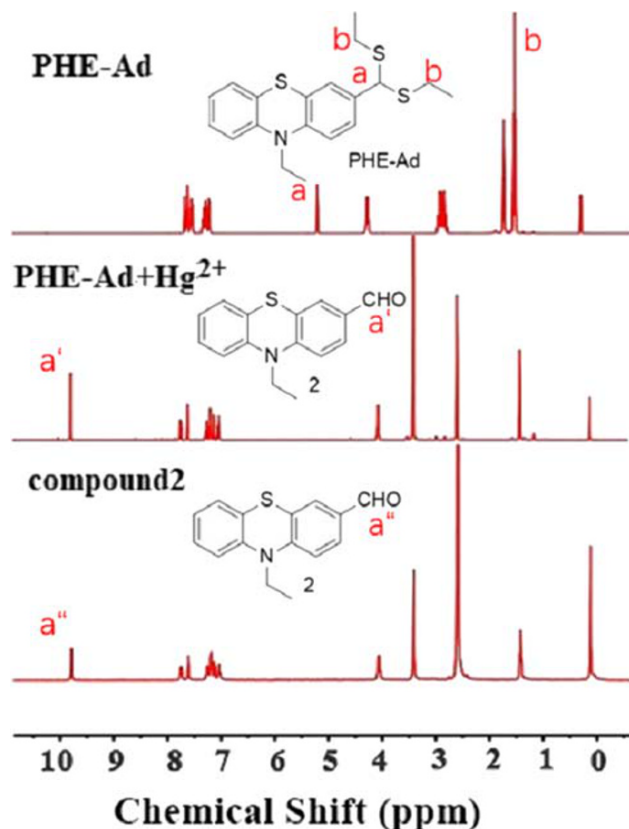


**FIGURE 9** <sup>1</sup>H NMR spectrum of the product of the deprotection reaction between the compound PHE-Ad and Hg<sup>2+</sup>

fluorescence intensity did not change significantly at 610 nm. After Hg<sup>2+</sup> was added to the above mixed solution, the fluorescence emission intensity was significantly enhanced at 610 nm (Figure 10). The above results show that the compound PHE-Ad has good anti-interference ability.

### 3.9 | Effect of pH

Compounds are affected by pH when they undergo chemical reactions. In order to find the most suitable pH range for Hg<sup>2+</sup> detection, a series of studies have been conducted on the effect of pH on fluorescence performance. The fluorescence intensity gradually increased in the range of pH 2.0–5.00, the fluorescence intensity reached the maximum value at pH 5.0–9.0, and the fluorescence intensity decreased gradually at pH 9.0–12.0 (Figure 11). The results show that the compound has a good detection ability for Hg<sup>2+</sup> in the range of pH 5.0–9.0, therefore, it can be applied to physiological detection.

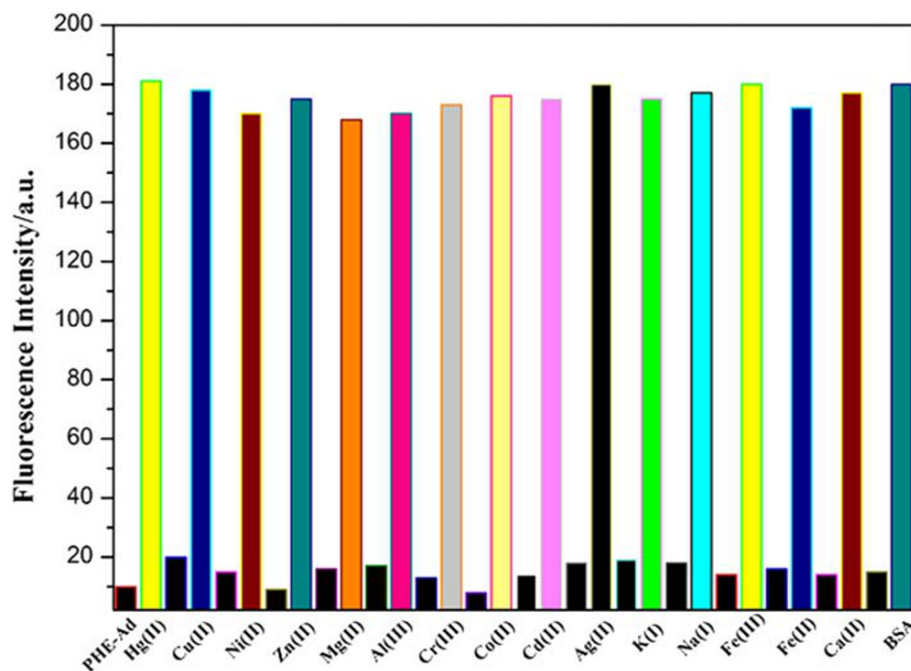


**FIGURE 10** Fluorescence emission intensity diagram of compound PHE-Ad under different metal ions

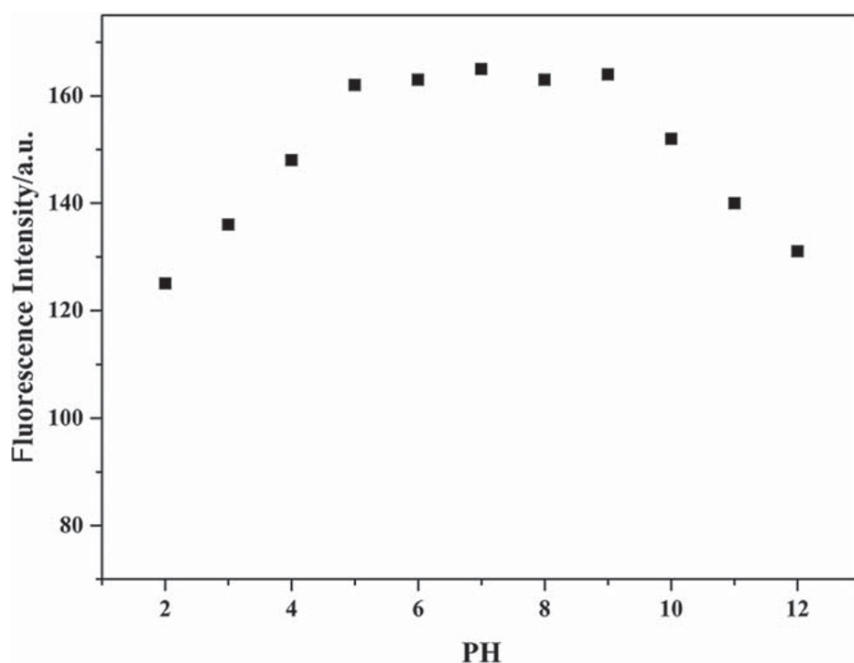


**FIGURE 11** Fluorescence emission intensity diagram of compound PHE-Ad at different pH values

### 3.10 | Reaction time on sensing $\text{Hg}^{2+}$

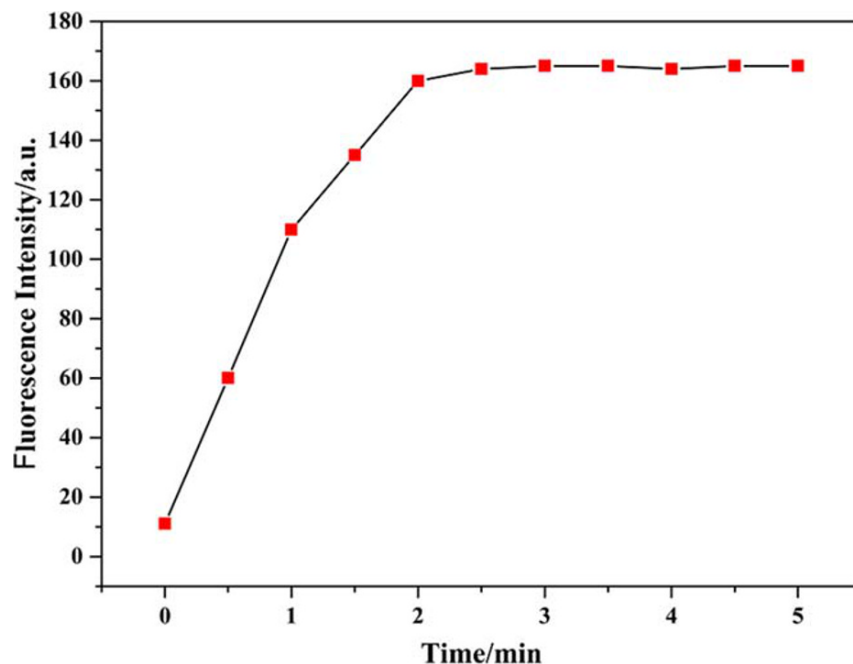
The short response time is a key factor for a designed sensor, therefore, the time dependent fluorescence responses of PHE-Ad toward  $\text{Hg}^{2+}$  were investigated in EtOH/ $\text{H}_2\text{O}$  (1:1, v/v) solution. The fluorescence intensity gradually increases at 0–2 min, and the fluorescence intensity does not change after 2 min. The results show that the reaction is completely completed within 2 min, therefore, the fluorescence performance test should be performed after

the PHE-Ad reacts with  $\text{Hg}^{2+}$  for 2 min under mild conditions and without any catalyst (Figure 12). Therefore, PHE-Ad probes have the advantages of rapid response and short response time.

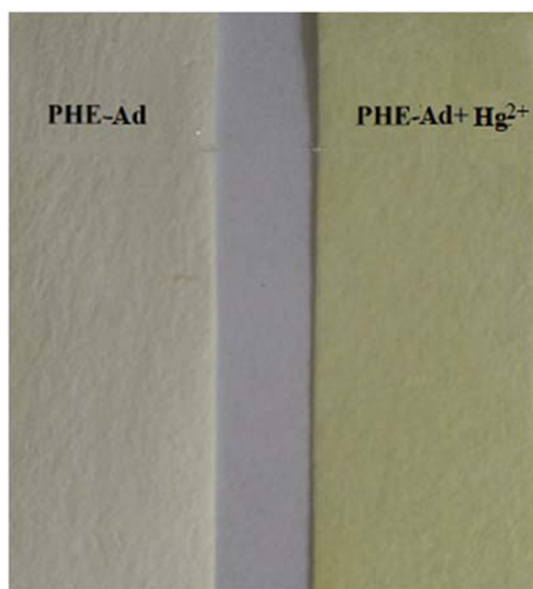
### 3.11 | Sensor PHE-ad-based test strips

In order to determine whether the compound fluorescent probe can effectively detect  $\text{Hg}^{2+}$  as a solid colorimetric



**FIGURE 12** Time-dependent of the fluorescence intensity

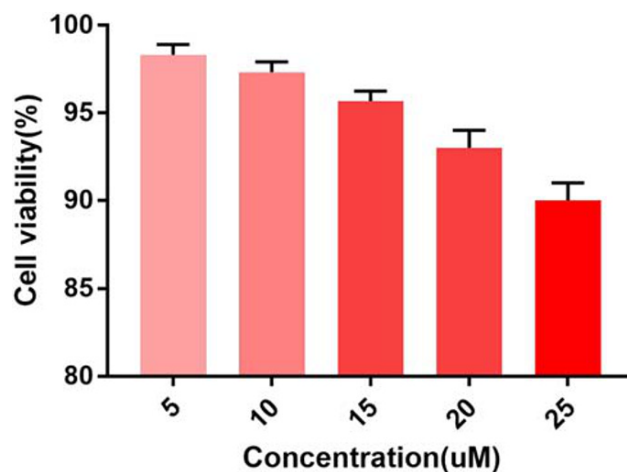
reagent, the recognition ability of the compound was studied on a filter paper test strip. The filter paper strip was placed in a compound concentration of  $1.0 \times 10^{-3}$  mol/l DMSO solution for a few seconds, then taken out and air-dried. Then, the dried filter paper strip was put into a  $\text{Hg}^{2+}$  aqueous solution having a concentration of  $1.0 \times 10^{-5}$  mol/l. When the filter paper strip is placed in the  $\text{Hg}^{2+}$  aqueous solution, the color of the filter paper strip changes rapidly from colorless to yellow, and the color of the filter paper strip does not change when other metal ion solutions are placed (Figure 13).

**FIGURE 13** Photographs showing the color changes of sensor PHE-Ad before and after addition of  $\text{Hg}^{2+}$ 

The above results show that PHE-Ad can be used as a solid indicator to detect  $\text{Hg}^{2+}$  in aqueous solution. Therefore, the PHE-Ad could be conveniently handled at any moment for the selective colorimetric detection of  $\text{Hg}^{2+}$  by the naked eye.

### 3.12 | Cellular imaging of $\text{Hg}^{2+}$

Inspired by the excellent “turn-on” fluorescent sensing behavior of sensor PHE-Ad for  $\text{Hg}^{2+}$ , the cellular imaging capability in living HeLa cells was further studied. Firstly, the cytotoxicity of PHE-Ad towards HeLa cells at different concentrations (0 ~ 25  $\mu\text{M}$ ) was tested using

**FIGURE 14** Cellular activity of PHE-Ad against HeLa cells at different concentrations (0–25  $\mu\text{M}$ )

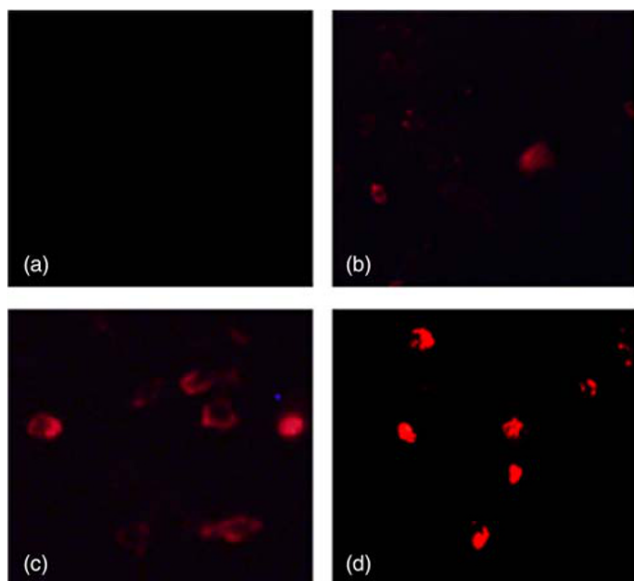


**FIGURE 15** a-d (a) Fluorescent image of HeLa cells with PHE-Ad for 1 hr; (b) Fluorescent images of HeLa cells incubated with PHE-Ad and  $\text{Hg}^{2+}$  ( $5 \mu\text{M}$ ) for 1 hr; (c) Fluorescent images of HeLa cells incubated with PHE-Ad and  $\text{Hg}^{2+}$  ( $15 \mu\text{M}$ ) for 1 hr; (d) Fluorescent images of HeLa cells incubated with PHE-Ad and  $\text{Hg}^{2+}$  ( $25 \mu\text{M}$ ) for 1 hr

MTT assay (Figure 14). The test results show that PHE-Ad has low cytotoxicity to living cells, and even at high concentrations, the cell viability is still above 90% within 24 hr. Then, HeLa cell imaging experiments were measured with a sensor PHE-Ad at a concentration of  $10 \mu\text{M}$ . Sensor PHE-Ad alone incubated for 60 min did not fluoresce in the relevant area (Figure 15). Next, HeLa cells were first incubated with PHE-Ad for 60 min, and then excess sensors that did not enter the cells were washed away. Then different concentrations of  $\text{Hg}^{2+}$  were added and incubated for 30 min, then clear green fluorescence was observed. As the mercury ion concentration increases, the cells showed stronger fluorescence (Figure 15bcd). Therefore, these cell imaging results demonstrated that sensor PHE-Ad could effectively image  $\text{Hg}^{2+}$  in living cells.

### 3.13 | Practical application research

In order to study the actual detection ability of PHE-Ad, it was added to drinking water containing  $\text{Hg}^{2+}$ . When the compound PHE-Ad was added to drinking water, no color change occurred. When the compound PHE-Ad and  $\text{Hg}^{2+}$  were added to drinking water, the color of the drinking water changed from colorless to yellow. The above results show that the compounds have potential application value in practical environmental detection (Figure 16).



**FIGURE 16** Drinking water colorimetric detection chart

## 4 | CONCLUSION

In summary, we developed a new phenothiazine-based sensor PHE-Ad based on the ICT mechanism and proved to have high applicability, low detection limit and easy-to-handle. It has particularly excellent detection capabilities in the appropriate working pH range. Due to the excellent performance of PHE-Ad, it has been successfully applied to the detection and imaging of  $\text{Hg}^{2+}$  in the environment and its drinking water, test paper and living cells, which has provided a convenient, reliable and accurate method for  $\text{Hg}^{2+}$  analysis. This probe overcomes the limitations of the probes reported so far, and has been used to image  $\text{Hg}^{2+}$  in environmental samples and cells, rather than the detection of a single environment.

## ACKNOWLEDGEMENTS

The work was supported by the Shandong Provincial Natural Science Foundation of China (ZR2017LC005, ZR2018PB007), the Major Science and Technology Innovation Project of Shandong Province (2018 CXGC1107).

## AUTHOR CONTRIBUTIONS

**Yucheng Sun:** Conceptualization; data curation; formal analysis; investigation; resources. **Lizhen Wang:** Methodology; validation. **Jianhua Zhou:** Data curation; investigation; resources. **Dawei Qin:** Formal analysis;

investigation; resources. **Hongdong Duan:** Funding acquisition; supervision.

## ORCID

Hongdong Duan  <https://orcid.org/0000-0002-0731-6732>

## REFERENCES

- [1] Z.-Y. Gao, C.-J. Zhang, X. Zhang, S. Xing, J.-s. Yao, C.-d. Qiao, *J. Mol. Struct.* **2019**, 1188, 14.
- [2] S. K. Patil, D. Das, *Spectrochim. Acta, Part a* **2019**, 210, 44.
- [3] A. I. Said, N. I. Georgiev, V. B. Bojinov, *Dyes Pigm.* **2019**, 162, 377.
- [4] X. Jiao, Z. Xiao, P. Hui, C. Liu, Q. Wang, X. Qiu, S. He, X. Zeng, L. Zhao, *Dyes Pigm.* **2019**, 160, 633.
- [5] S. L. Shen, X. Q. Huang, X. H. Lin, X. Q. Cao, *Anal. Chim. Acta* **2019**, 1052, 124.
- [6] B. B. Correia, T. R. Brown, H.-S. Lee, J. H. Reibenspies, R. D. Hancock, *Polyhedron* **2020**, 179, 114366.
- [7] Y. Song, Y. Zheng, S. Zhang, Y. Song, M. Niu, Y. Li, Z. Ye, H. Yu, M. Zhang, Y. Xiao, *Sens. Actuators, B* **2019**, 286, 32.
- [8] V. V. Annenkov, S. N. Zelinskiy, V. A. Pal'shin, L. I. Larina, E. N. Danilovtseva, *Dyes Pigm.* **2019**, 160, 336.
- [9] T. Anand, S. K. A. Kumar, S. K. Sahoo, *Spectrochim. Acta a* **2018**, 204, 105.
- [10] M. Hong, Y. Chen, Y. Zhang, D. Xu, *Analyst* **2019**, 144, 7351.
- [11] Y. Chen, X. Shi, Z. Lu, X. Wang, Z. Wang, *Anal. Chem.* **2017**, 89, 5278.
- [12] J. Y. Liang, L. Han, S. G. Liu, Y. J. Ju, N. B. Li, H. Q. Luo, *Spectrochim. Acta a* **2019**, 222, 117260.
- [13] S. W. Cho, A. S. Rao, S. Bhunia, Y. J. Reo, S. Singha, K. H. Ahn, *Sensor Actuat B-Chem.* **2019**, 279, 204.
- [14] E. Dhineshkumar, M. Iyappan, C. Anbuselvan, *J. Mol. Struct.* **2019**, 1177, 545.
- [15] M. E. Aliaga, M. Gazitua, A. Rojas-Bolanos, M. Fuentes-Estrada, D. Durango, O. Garcia-Beltran, *Spectrochim. Acta a* **2020**, 224, 117372.
- [16] C. Liu, A. Tuffour, J. Liao, M. Li, Q. Lv, D. Zhou, L. Gao, *Chem. Phys.* **2020**, 534, 110758.
- [17] X. Jiao, C. Liu, S. He, L. Zhao, X. Zeng, *Dyes Pigm.* **2019**, 160, 86.
- [18] H. Chen, P. Yang, Y. Li, L. Zhang, F. Ding, X. He, J. Shen, *Spectrochim. Acta, Part a* **2020**, 224, 117384.
- [19] H. Mohammad, A. S. M. Islam, C. Prodhan, M. Ali, *New J. Chem.* **2019**, 43, 5297.
- [20] M. Phichi, A. Imyim, T. Tuntulani, W. Aeungmaitrepirom, *Anal. Chim. Acta* **2020**, 1104, 147.
- [21] A. S. Murugan, N. Vidhyalakshmi, U. Ramesh, J. Annaraj, *Sensor Actuat B-Chem.* **2018**, 274, 22.
- [22] J. Qiu, S. Jiang, B. Lin, H. Guo, F. Yang, *Dyes Pigm.* **2019**, 170, 107590.
- [23] S. Adhikari, S. Ta, A. Ghosh, S. Guria, A. Pal, M. Ahir, A. Adhikary, S. K. Hira, P. P. Manna, D. Das, *J. Photochem. Photobiol., a* **2019**, 372, 49.
- [24] P. Yin, Q. Niu, Q. Yang, L. Lan, T. Li, *Tetrahedron* **2019**, 75, 130687.
- [25] S. Erdemir, *Sens. Actuators, B* **2019**, 290, 558.
- [26] C. Xu, C. Xin, C. Yu, M. Wu, J. Xu, W. Qin, Y. Ding, X. Wang, L. Li, W. Huang, *Chem. Commun.* **2018**, 54, 13491.
- [27] S. J. Bora, R. Dutta, S. Ahmed, D. J. Kalita, B. Chetia, *J. Mol. Struct.* **2019**, 1194, 178.
- [28] L. Yan, D. Nan, C. Lin, Y. Wan, Q. Pan, Z. Qi, *Spectrochim. Acta, Part a* **2018**, 202, 284.
- [29] J. Li, F. Huo, Z. Wen, C. Yin, *Spectrochim Acta a* **2019**, 221, 117156.
- [30] X. Han, C. Tian, M. S. Yuan, Z. Li, W. Wang, T. Li, S. W. Chen, J. Wang, *Anal. Chim. Acta* **2019**, 1052, 137.
- [31] K. Zhong, L. Chen, Y. Pan, X. Yan, S. Hou, Y. Tang, X. Gao, J. Li, L. Tang, *Spectrochim Acta a* **2019**, 221, 117135.
- [32] X. Jin, X. Wu, B. Wang, P. Xie, Y. He, H. Zhou, B. Yan, J. Yang, W. Chen, X. Zhang, *Sens. Actuators, B* **2018**, 261, 127.
- [33] X. Zhang, B. Wang, Y. Xiao, C. Wang, L. He, *Analyst* **2018**, 143, 4180.
- [34] L. L. Fengli Gao, J. Fan, J. Cao, Y. Li, L. Chen, X. Peng, *Anal. Chem.* **2019**.
- [35] X. Leng, X. Jia, C. Qiao, W. Xu, C. Ren, Y. Long, B. Yang, *J. Mol. Struct.* **2019**, 1193, 69.
- [36] S. Wang, Z. Li, Y. Liu, G. Feng, J. Zheng, Z. Yuan, X. Zhang, *Sens. Actuators, B* **2018**, 267, 403.
- [37] D. Vashisht, K. Kaur, R. Jukaria, A. Vashisht, S. Sharma, S. K. Mehta, *Sensor Actuat Chem B-* **2019**, 280, 219.
- [38] K. Xu, Y. Li, Y. Si, Y. He, J. Ma, J. He, H. Hou, K. Li, *J. Lumin.* **2018**, 204, 182.
- [39] G. Yang, X. Meng, S. Fang, L. Wang, Z. Wang, F. Wang, H. Duan, A. Hao, *New J. Chem.* **2018**, 42, 14630.
- [40] C. Wang, L. Wang, S. Fang, D. Qin, J. Zhou, G. Yang, S. Jin, H. Duan, **2019**.

**How to cite this article:** Sun Y, Wang L, Zhou J, Qin D, Duan H. A new phenothiazine-based fluorescence sensor for imaging Hg<sup>2+</sup> in living cells. *Appl Organomet Chem.* 2020;e5945. <https://doi.org/10.1002/aoc.5945>